CHEMISTRY
A EUROPEAN JOURNAL

DOI: 10.1002/chem.200600103

Characterising the Electronic Structure of Ionic Liquids: An Examination of the 1-Butyl-3-Methylimidazolium Chloride Ion Pair

Patricia A. Hunt,*[a] Barbara Kirchner,[b] and Tom Welton[a]

Abstract: In this paper we analyse the electronic properties of gas-phase 1-butyl-3-methylimidazolium Cl ion pairs, $[C_4C_1im]Cl$, in order to deepen our understanding of ionic liquids in general. Examination of charge densities, natural bond orbitals (NBO), and delocalised molecular orbitals computed at the B3LYP and MP2/6-31++G(d,p) levels have enabled us to explain a number of experimental phenomena: the relative acidity of different sites on the imidazolium ring, variations in hydrogen-bond donor and acceptor abilities, the apparent contradiction of the hydrogen-bond-donor parameters for different types of solute, the low probability of finding a Cl^- anion at the rear of the imidazolium ring and the expansion of the imidazolium ring in the presence of a strong hydrogen-bond acceptor. The unreactive but coordinating environment and large electrochemical window have also been accounted for, as has the strong electron-donating character of the carbon atoms to the rear of the ring in associated imidazolylidenes. The electronic structure of the $[C_4C_1im]^+$ cation is best described by a $C^4{=}C^5$ double bond at the rear, and a delocalised three-centre $4e^-$ component across the front (N^1-C^2-N^3) of the imidazolium ring; delocalisation between these regions is also significant. Hydrogen-bond formation is driven by Coulombic stabilisation, which compensates for an associated destabilisation of the electronic part of the system. Interactions are dominated by a large positive charge at C^2 and the build up of π-electron density above and below the ring, particularly that associated with the double bond between C^4 and C^5. The NBO partial charges have been computed and compared with those used in a number of classical simulations.

Keywords: ab initio calculations · electronic structure · hydrogen bonds · ionic liquids

Introduction

Room-temperature ionic liquids (ILs) exhibit interesting and sometimes unusual physical properties, such as vanishing vapour pressure, a large liquidus range, high thermal stability, high ionic conductivity, high electrochemical stability and favourable solvation behaviour. Much of the interest in ionic liquids has been driven by their use in synthesis and catalysis.[1–3] A key feature of ionic liquids is the large number of ion combinations that are possible,[4] which opens up the possibility of altering the constituent ions in order to tailor to particular physical and chemical properties.

In order to design ionic liquids, predict their physical properties or even choose one (out of the trillions) suitable for a specific reaction it is necessary to make a link between the fundamental properties of the system (such as electronic and molecular structure) and specific (macromolecular) physical and chemical properties. In room-temperature ionic liquids there is a complex interplay of forces—Coulombic, dipole–dipole, dipole-induced dipole, dispersion and hydrogen bond—which has yet to be unravelled. Before solvation in ionic liquids can be understood, we need to have an awareness of the electronic interactions occurring in the pure solvent.

We are interested in the electronic structure of ionic liquids, and have undertaken a detailed study of ion pairing for the prototypical ionic liquid 1-butyl-3-methylimidazolium

[a] Dr. P. A. Hunt, Prof. T. Welton
Chemistry Department
Imperial College London
London, SW7 2AZ (UK)
Fax (+44) 207-594-5850
E-mail: p.hunt@imperial.ac.uk

[b] Dr. B. Kirchner
Institut für Physikalische und Theoretische Chemie
Universität Bonn
Wegelerstrasse 12, 53115 Bonn (Germany)

Supporting information for this article is available on the WWW under http://www.chemeurj.org/ or from the author. It contains a figure showing the ion pair partial-charge distribution, a table comparing selected charges from the front-meth-1a and front-meth-1b conformers of $[C_4C_1im]Cl$, and plots of the LUMO, HOMO, HOMO−1, and HOMO−3 of the front-meth-1a ion pair.

chloride, of which 1-butyl-3-methylimidazolium (Scheme 1) is a typical ionic-liquid cation. Recently, a $[C_nC_m\text{im}]^+$ notation (where n and m indicate the number of carbon atoms in the alkyl chains at N^1 and N^3, respectively) has been used

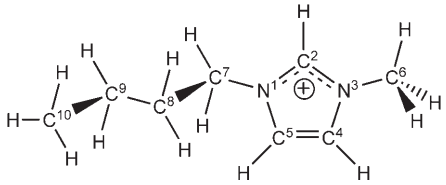

Scheme 1. The 1-butyl-3-methylimidazolium cation, $[C_4C_1\text{im}]^+$.

in naming imidazolium cations and this will be used in the present paper.[5] An understanding of the electronic structure of the components and ion-pairing interactions will help us to understand the local forces acting on individual molecules within an ionic liquid. If a relationship can be found between the gas-phase electronic structure and the experimentally observed behaviour, ab initio computational studies of simple ion pairs can be used to understand and predict selected features of ionic liquids, and thus could be used to guide the choice of an appropriate pairing before significant investment is made in synthesis and physical characterisation.

The electronic structure of the aromatic imidazolium cation is not well defined, and is often represented as shown in Figure 1. The imidazolium ring is assumed to be aromatic and the positive charge is fully delocalised on the ring (Figure 1a). The dominant resonance structures (Figure 1b and c) have the positive charge "formally" carried by the quaternary nitrogen atoms. A minor resonance structure with C^2 carrying a positive charge is also possible (Figure 1d). The electron distribution can also be represented as shown in Figure 1e. The electronic nature of the imidazolium cations has not been investigated in any depth. Questions that arise include, where is the positive charge, how delocalised is the electron density and what impact does this have on the acidity of the imidazolium ring hydrogen atoms?

The imidazolium cation ($A{-}H^+$) is isoelectronic with the imidazolylidene (or N-heterocyclic) carbene (A), shown in Figure 2. Since the first stable free N-heterocyclic carbene was isolated by Arduengo et al. in 1991, there has been substantial theoretical interest in defining the electronic structure of these N-substituted ylidene compounds.[6–14] Two different bonding models have been advanced for the imidazolylidenes. One model proposes that there is substantial σ-

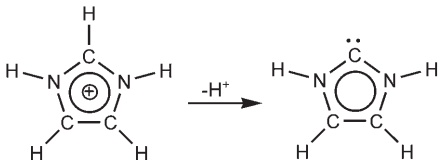

Figure 2. The unsubstituted imidazole cation and imidazole-2-ylidene.

electron charge transfer from the carbenic C atom to the adjacent N atoms, with only minor π-electron effects.[7] Here, the N-heterocyclic carbene is kinetically stabilised owing to electron repulsion between the lone pair at the carbene and those on the adjacent nitrogen atoms.[14] This is supported by charge densities and topological analysis, which show little evidence of cyclic delocalisation. The second model proposes that π-electron donation from the nitrogen lone pairs into the empty carbene-type carbon p_π orbital is dominant, and considers cyclic delocalisation to be significant.[8] This is supported by thermodynamic, magnetic, and structural data. The cations $A{-}H^+$ are expected to exhibit significantly more π-electron delocalisation than their carbene analogues.[9] Although the electronic structure of carbenes has been extensively investigated, and there is a substantial body of information on the carbenes that can be drawn upon in analysing imidazolium cations, the cations themselves have been neglected.

Some insight into the electronic properties of ionic liquids has also been obtained by using spectroscopic probe methods, for example, with the Kamlet–Taft parameters, which describe the polarisability (π^*), hydrogen-bond donor (acidity, α) and hydrogen-bond acceptor (basicity, β) properties of solvents.[15–19] However, recent experiments evaluating the hydrogen-bond acidity of the imidazolium-based ILs have produced contradictory results and have led to some confusion. In solvatochromic experiments using Reichardt's dye as a probe, $[C_4C_1\text{im}]^+$-based ionic liquids were shown to be good hydrogen-bond donors with α values of approximately 0.62.[19] However, in complementary gas chromatography (GC)-based experiments using a number of small probe molecules, the same $[C_4C_1\text{im}]^+$-based ionic liquids were shown to be poor hydrogen-bond donors.[20] We believe we have resolved this apparent contradiction.

The relative acidity of the hydrogen atoms in the imidazolium ring, particularly that at C^2, is important for quantifying the effect of an IL on a potential solute. Experimental evidence strongly suggests that the hydrogen atom at C^2 (C^2–H) is more acidic than those at C^4 or C^5 ($C^{4/5}$–H).[19,21–23] Theoretical calculations on deprotonation of unsubstituted

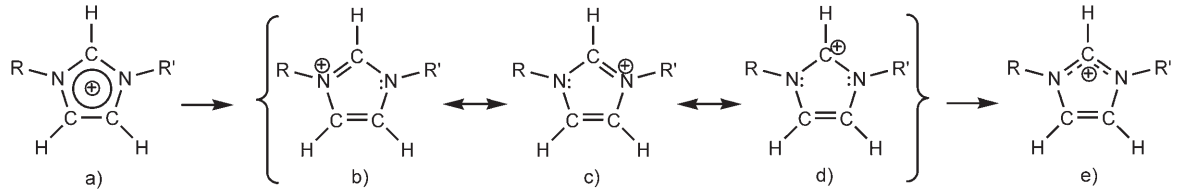

Figure 1. Representations of the imidazolium $[C_4C_1\text{im}]^+$ cation electronic structure indicating the formal assignment of charges.

imidazolium cations have predicted pK_a values of 24.90 and 32.97 for the C^2–H and $C^{4/5}$–H hydrogen atoms, respectively.[11] However, there is also experimental evidence that imidazolium salts will, under certain conditions, prefer to bind to transition metals at $C^{4/5}$, that is, at the less-acidic sites.[24] We therefore investigated the acidity of the C^2–H versus $C^{4/5}$–H sites as interpreted through computational indicators. Moreover, the $C^{4/5}$-bound carbenes have been found to be more electron donating than their C^2 analogues, evidence that hydrogen-atom acidity is not the only important electronic property for imidazolium-based ILs.[25,26] We will explain why the imidazolylidene coordinated through $C^{4/5}$ appears to be more electron donating relative to that coordinated through C^2.

A range of theoretical methods have now been used to investigate ILs. Classical molecular dynamics (MD) and Monte Carlo methods have been used to investigate, primarily, the neat imidazolium-based ionic liquids (and particularly $[C_4C_1im][PF_6]$).[27–40] These have provided insight into the average arrangement of ions in the pure ionic liquids and for solvated species, as well as providing theoretical predictions of thermodynamic properties. The success of an MD simulation depends on the quality of the inter- and intramolecular potential functions and on the charges associated with each atom or group.[39,41] One of the drawbacks of (nonpolarisable) classical methods is the sheer variety of charges and potentials that can be used. This problem has been highlighted recently for ionic liquids and $[C_4C_1im]Cl$ in particular.[37–39] Across different classical models the nitrogen atoms of the imidazolium cation have varied from being significantly negative ($-0.4e$) through essentially zero ($+0.05e$) to mildly positive ($+0.15e$). A significant problem at this point is the validation of any given classical IL model,[38] and ab initio quantum-chemical studies can provide a valuable point of reference. The electronic structure is accurately represented by good quality ab initio calculations and these can be used to evaluate the lower-level electronic structures used to determine the parameters for use in classical simulations. We have carried out a natural bond orbital (NBO) analysis of the MP2 density, which we believe provides a useful reference point for an analysis of the charge distribution in this IL.

There are still relatively few ab initio quantum-chemical calculations on the gas-phase ion pairs that make up ionic liquids. Moreover, many of these studies have concentrated on geometries and neglected to further analyse the electronic wave function or density. Early studies on ionic liquids are limited to the chloroaluminate melts.[42–47] A number of studies treat isolated imidazolium cations but have primarily been directed toward producing parameters for use in force fields.[36,38,39,48] More recently, imidazolium-based ionic liquids have been examined in which the anion has been one or more of a halide, $[BF_4]^-$, $[BPh_4]^-$, $[PF_6]$ or $[CF_3CO_2]^-$.[49–56] Ab initio MD methods have only very recently been employed to examine $[C_1C_1im]Cl$.[41,57,58] Such calculations show that the gross structure of the liquid is captured by classical MD simulations, but that the details, such as the anion position in the first solvation shell of the cation, are different.[41,57] The use of density functional theory (DFT) methods can be problematic due to the neglect of dispersion effects, which impact on the ability to accurately describe configurations in which the anion sits above or below the aromatic imidazolium ring.[41,56] Bühl and co-workers recently examined the electronic structure of the periodic system by using population analysis methods and maximally localised Wannier functions.[41]

This work reports on an analysis of the electronic structure of the $[C_4C_1im]Cl$ ion pair, and is aimed at deepening our understanding of the electronic effects that lead to the physico-chemical properties of ionic liquids. The paper is organised as follows: The electronic structure of the isolated $[C_4C_1im]^+$ cation, and then the $[C_4C_1im]Cl$ ion pair are explored by using population analysis tools, electron density maps, Laplacian plots, and orbital analysis (including localised natural bond orbitals and delocalised molecular orbitals). An attempt is then made to connect these results with the experimentally determined polarisability, hydrogen-bond donor and acceptor properties and observed relative acidities and reactivity of ILs. Finally, a comparison is made between the atomic charges determined here from the NBO and Mulliken population analysis and those used in recent classical simulations. Our results and deductions are summarised in the concluding section. The methods and basis sets employed are summarised in the Computational Methods section.

Results and Discussion

Electronic structure

The $[C_4C_1im]^+$ cation: The atomic structure of the $[C_4C_1im]^+$ cation is given in Scheme 1. Butyl chain rotation in the cation is facile and has been found to vary over a large range of angles for little cost in energy. Three low-energy $[C_4C_1im]^+$ cation conformers, cation-a, cation-b and cation-c, have previously been determined by us (Figure 3).[56] These conformers lie within 2.7 kJ mol^{-1} of each other at the B3LYP/6-31++G(d,p) level. The relative-energy ordering varies with the basis set and the amount of correlation included in a calculation.

Partial charges: The NAO charges for the lowest-energy $[C_4C_1im]^+$ cation, cation-a, are presented in Table 1. The essential features of this charge distribution are represented in Figure 4, in which the atomic charges are listed except for the butyl chain for which the group charges are shown. A primary feature of the NAO charge distribution is that most of the positive charge is located on the peripheral H atoms. An alternating chain of charge through the front of the aromatic ring, C^7-N^1-C^2-N^3-C^6, results in a significant positive charge on the C^2–H unit, and a significant negative charge on the N atoms. Atoms $C^{4/5}$ remain essentially neutral. Of particular interest is the "acidity" of the H atoms on the

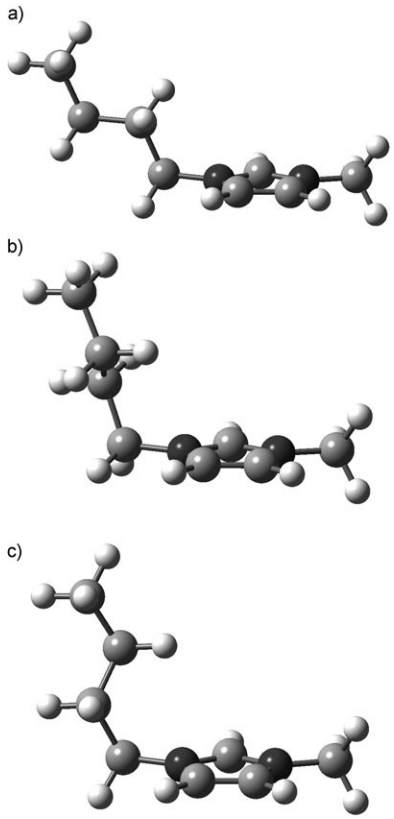

Figure 3. Three low-energy $[C_4C_1im]^+$ cation conformers: a) cation-a, b) cation-b, and c) cation-c.

Table 1. Selected charges from the natural atomic orbital (NAO) analysis of the $[C_4C_1im]^+$ cation.

	B3LYP	MP2
N_1	−0.341	−0.324
N_3	−0.348	−0.327
C_2	0.268	0.235
C_4	−0.039	−0.035
C_5	−0.035	−0.037
C_6	−0.449	−0.421
C_7	−0.241	−0.225
C_{10}	−0.661	−0.636
C_2–H	0.268	0.264
C_4–H	0.278	0.273
C_5–H	0.277	0.273

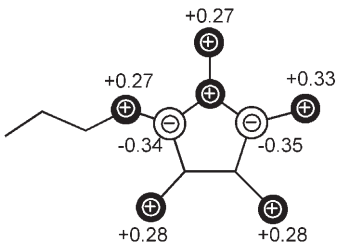

Figure 4. Charge pattern from the NAO analysis of the $[C_4C_1im]^+$ cation. The specified alkyl charges are methylene and methyl group charges (not atomic charges). No charge indicates an essentially neutral group.

ring; the charge is essentially the same for all of these H atoms. Bühl et al. also noticed that $C^{4/5}$–H and C^2–H carry similar charges in the $[C_1C_1im]^+$ cation.[41] This simple indicator suggests that C^2–H is no more or less acidic than $C^{4/5}$–H, and contradicts a wealth of experimental data showing that the C^2–H hydrogen atom is the most acidic in the ring.[19,21,22] However, although the H atoms are connected to essentially neutral C atoms at $C^{4/5}$, the H atom is bound to a positively charged C atom at C^2. A statistical correlation has previously been found between the combined charge on an X–H (X = N, O) moiety and the hydrogen-bond donor ability of a compound.[59] The B3LYP/6-31++G(d,p) $[C_4C_1im]^+$ cation charges are $q(C^2\text{–H}) = +0.536$, $q(C^4\text{–H}) = +0.239$ and $q(C^5\text{–H}) = +0.242$. Thus, the relative acidity of the ring hydrogen atoms should not be associated with the H atoms alone, but with the charge on the "C^n–H" moiety. When this is carried out, agreement with experimental observations is achieved.

The carbon atoms of the alkyl chain are negatively charged, except for those adjacent to the imidazolium ring. Summing the positive hydrogen atom charges into the heavy atoms (such as carbon) leaves roughly neutral methyl or methylene groups, and hence van der Waals forces rather than Coulombic forces begin to dominate in alkyl chains. The NAO analysis of the more sophisticated MP2/6-31++G(d,p) density is very similar to that obtained at the B3LYP level, indicating that the inclusion of dispersion effects is not crucial to providing a good representation of the charge density. The main difference between these charge distributions is a slight reduction in the charge polarisation on the heavy atoms of the imidazolium ring, indicating a slightly enhanced aromatic character.

Bonding analysis: Each of the resonance structures shown in Figure 1 has been examined by using the NBO analysis tools. The greater the non-Lewis character the smaller contribution a resonance structure is expected to make to the overall electronic structure. The non-Lewis character for the three resonance structures depicted is 1.55% (N^3 lone pair), 1.56% (N^5 lone pair) and 2.11% (C^2 positively charged), indicating that the structures with a single nitrogen lone pair are almost, but not quite, equivalent and that the structure with a positive charge on C^2 contributes only slightly less. The importance of this final resonance structure to the overall electronic description is indicated by the significant positive charge determined for C^2.

The extent of delocalisation in the imidazolium cation is also of interest. Formally, there are six p_π electrons to be shared over five p_π orbitals. Boehme and Frenking pointed out that if the six p_π ring electrons were equally distributed over the ring atoms, each would have 1.2 π electrons. The occupancy of the formally empty C^2 p_π orbital can therefore be used to give an indication of the extent of delocalisation.[8] They established that the unsubstituted imidazol-2-ylidene has 55.8% of a perfectly delocalised π system; by using this criteria the $[C_4C_1im]^+$ cation exhibits a very high level of delocalisation of 80.3%.

However, the extent of delocalisation around the entire ring is less clear. NBO analysis determines a double bond between C^4 and C^5, and thus there remains a three-centre (N^1-C^2-N^3) four-electron (3c-4e) π system. Clearly, the last two electrons must enter into a π-type antibonding orbital. Hence, any addition of electrons to this system will result in increased antibonding and destabilisation of the electronic structure. The higher electronegativity of the nitrogen atoms relative to the carbon atoms ensures that electrons are not equally distributed along N^1-C^2-N^3. In keeping with the fact that σ induction favours "pushing" more electron density onto the more electronegative nitrogen atoms, analysis of the carbon–nitrogen σ bonds showed that they are ≈63% nitrogen based. The corresponding carbon–nitrogen π bonds ($\pi_{C=N}$) are ≈70% nitrogen based. However, there is also significant occupation of the C^2–N^1 π* bond (0.54*e*), which (because of its antibonding nature) is primarily polarised (≈70%) onto the carbon atom, thus "pulling" electron density away from the nitrogen atoms. Hence, σ induction and π delocalisation result in significant push–pull effects on the electron density and indicate that there is substantial delocalisation through the N^1-C^2-N^3 part of the ring. Given the charges determined for C^2 (+0.268) and N atoms (−0.346), σ-inductive effects dominate.

Figure 5a shows the NBO HOMO–LUMO region for the most-stable resonance structure (N^3 lone pair). The $\pi^*_{C=N}$ lies lower in energy than the $\pi^*_{C=C}$ bond orbital and thus is more heavily occupied. A second-order estimate of the effect of delocalisation based on the occupation of the donating orbital, the orbital coupling and the energy difference

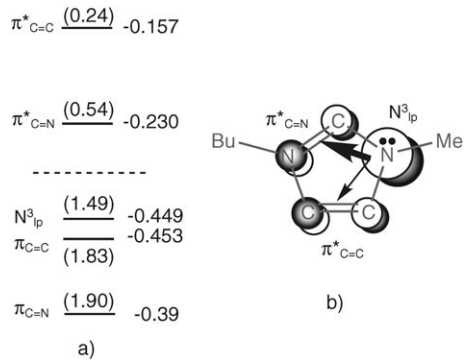

Figure 5. a) NBO HOMO–LUMO region of the $[C_4C_1im]^+$ cation. Orbital occupations are given in parentheses above or below each line, and orbital energies (atomic units) are given beside each line. b) Illustration of the primary delocalisation interactions.

between the coupled orbitals can be made by using the NBO analysis tools, and the primary interactions are presented in Table 2. The largest delocalisation components are from the N^3 lone-pair orbital (N^3_{lp}), and are depicted in Figure 5b. Delocalisation within the N^1-C^2-N^3 section totals 101.6 kJ mol^{-1}, while delocalisation to or from the C^4–C^5 section totals 79.0 kJ mol^{-1}, indicating that delocalisation is occurring around the entire ring, but that it is more extensive over the N^1-C^2-N^3 component.

Table 2. Primary delocalisation interactions occur from the orbitals in the "From" column to the orbitals in the "To" column.

From	To	Second-order energy [kJ mol^{-1}]
N^3_{lp}	$\pi^*_{C=N}$	77.80
N^3_{lp}	$\pi^*_{C=C}$	29.83
$\pi_{C=N}$	N^3_{lp}	22.77
$\pi^*_{C=N}$	$\pi^*_{C=C}$	17.09
$\pi_{C=N}$	$\pi^*_{C=C}$	16.87
$\pi_{C=C}$	$\pi^*_{C=N}$	15.24

The HOMO–LUMO gap has been associated with the hydrogen-bond capabilities of a molecule, however, in the case of $[C_4C_1im]Cl$ such an association would be misleading because hydrogen bonding requires the overlap of σ-type orbitals, and the HOMO and LUMO are π-type orbitals. The C–H σ-bond orbitals lie lower in energy and the C–H σ* orbitals lie much higher in energy. Moreover, it has been shown that the HOMO–LUMO gap does not statistically correlate with hydrogen-bond acidity (α).[59]

Analysis of the electron density: A contour plot of the Laplacian of $[C_4C_1im]^+$ in the N^1-C^2-N^3 plane is reproduced in Figure 6. Dashed lines indicate negative curvature of the electronic density, and thus areas where the local density is increasing (i.e., in bond regions between atoms). Gaps in the dashed contours as well as the solid contours indicate areas of local electron depletion. Areas of local acidity (loss of electron density) will be those favoured by nucleophilic attack, indicated by the arrows in Figure 6. Broad "wells"

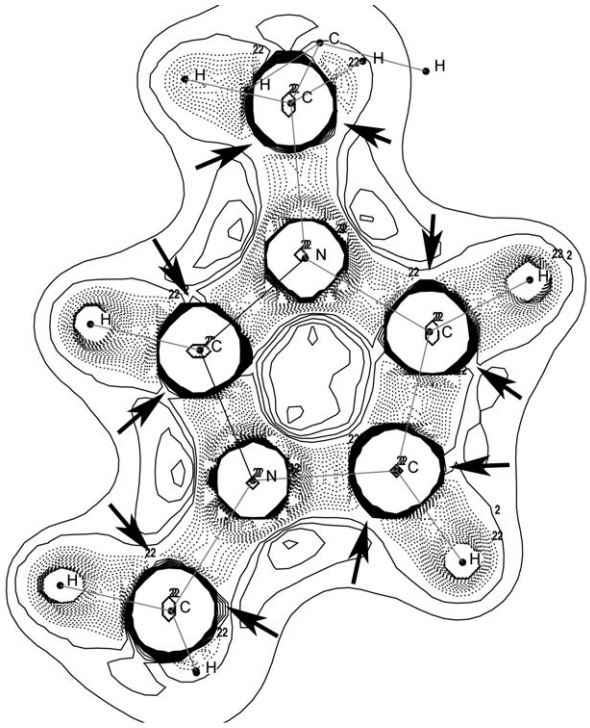

Figure 6. Contour map of the Laplacian projected onto the N^1-C^2-N^3 plane. Lines are positive and dashes are negative. Arrows indicate regions of local acidity on the ring C atoms.

where the electron density is decreasing exist either side of the alkyl groups, and "behind" the imidazolium ring; these will be favoured positions for the negatively charged Cl^- anion. The shallowness of the well between C^4 and C^5 indicates that an anion in this position will be less stable, which is consistent with the back conformer being about 60 kJ mol^{-1} higher in energy than the lowest-energy conformers.[56] It has also been found that the Cl^- anion does not align directly with the C–H bonds of the imidazolium ring, but sits slightly to the side, taking advantage of the local areas of electron depletion.

The ion pair [C_4C_1im]Cl: We, and others, have previously obtained multiple stable structures for the [C_4C_1im]Cl ion pair.[53,55,56] The chloride has seven possible locations, front-meth, front-but, top (and thus bottom), but-side, meth-side and back (Figure 7). The top and front conformers are the lowest in energy and almost degenerate. The meth-side and but-side conformers lie approximately 30 kJ mol^{-1}, and the back conformer approximately 60 kJ mol^{-1}, higher in energy

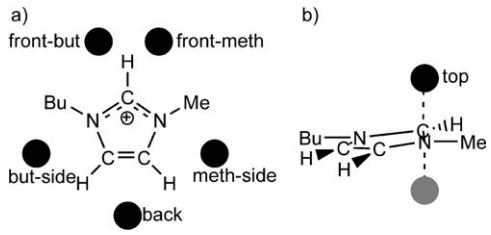

Figure 7. Location of primary cation–anion interaction sites for [C_4C_1im]Cl: a) Cl anion in-plane; b) Cl anion out-of-plane.

than the lowest-energy front conformer. Flat potential-energy surfaces in the locality of these minima indicate that motion of the chloride anion is facile.[56] In addition, as mentioned above, butyl chain rotation has been examined and found to vary over a large range of angles for little cost in energy.[37,39,56]

By using the information obtained from our analysis of the imidazolium cation we are able to rationalise the varying stability of these conformers. The Cl^- anion in the back conformer occupies a shallow potential-energy well, and, due to the essentially neutral $C^{4/5}$ moiety, it experiences minimal electrostatic attraction. In contrast, the Cl^- anion in the front or side conformers occupies a deeper potential-energy well. Due to the positive charge on C^2, the Cl^- anion in the front conformers experiences significantly greater electrostatic attraction, and due to the π bond between C^4 and C^5, the Cl^- anion in the side or back conformers experiences more electron–electron repulsion. The Cl^- anion is also stabilised by areas of local electron depletion, which occur between the substituents on the imidazolium ring, thus limiting the formation of linear hydrogen bonds. The regions of reduced electron density extend over quite a large area thus allowing the Cl^- anions to adjust relatively freely.

Partial charges: Selected partial charges for the dimers are reported in Table 3. The charge distribution in the cation of the dimer is qualitatively similar to that of the isolated ion. Essential features of the ion-pair distribution are represented in Figure S1 of the Supporting Information. Repositioning the Cl^- anion around the imidazolium ring has a discernable effect on the charge distribution in the ring. Rotation of the butyl chain, however, has only a very minor effect. Differences in selected NAO partial charges between front-meth-a and front-meth-b are given in the Supporting Information.

The Cl^- anion transfers charge to the cation, and the "extra" electron density is distributed over the N^1, N^3 and $C^{4/5}$-H centres. There is a rough correlation between the amount of charge transferred and the relative stability of each dimer pair: the more stable a dimer pair the more charge is transferred. Those hydrogen atoms that interact with the Cl^- anion become more positive, and the associated carbon atoms if they are C^{ring} become slightly less negative, or if they are C^{alkyl} become slightly more negative. The greater the positive charge at C^2 the more stable a conformer, but a decreasing charge on C^2 also means a decreasing p_π occupation and hence a reduction in aromaticity. Bühl et al. computed a charge transfer of 0.22*e* for [C_1C_1im]Cl.[41] Thus, on increasing the alkyl-chain length there has been a reduction in charge transfer to the imidazolium cation. Overall, the total amount of charge transferred is not large relative to charge movement within the cation, for example, the charge on the carbon atom of the butyl chain methyl group is ≈ -0.65. However, the charge transferred is more than that observed for some small neutral hydrogen-bonding molecules interacting with a closed shell Cl^- anion, for example, the charge on the Cl^- anion in $OH_2\cdots Cl^-$ and

Table 3. Selected partial charges, q, and Δq[a] from an NAO analysis of structures at the B3LYP/6-31++G(d,p) level for the "a-type" conformers.[b]

	front-meth	Δq	front-but	top	but-side	meth-side	back
Cl	−0.835	0.165	−0.840	−0.830	−0.877	−0.863	−0.928
N_1	−0.368	*−0.027*	−0.360	−0.356	−0.338	−0.356	−0.355
N_3	−0.361	−0.013	−0.373	−0.356	−0.365	−0.343	−0.359
C_2	0.272	0.004	0.277	0.292	0.242	0.238	0.222
C_4	−0.065	*−0.026*	−0.071	−0.057	−0.081	−0.017	−0.033
C_5	−0.062	*−0.027*	−0.056	−0.070	−0.017	−0.080	−0.031
C_6	−0.459	−0.010	−0.445	−0.475	−0.444	−0.474	−0.443
C_7	−0.231	0.010	−0.256	−0.244	−0.260	−0.237	−0.235
C_{10}	−0.659	0.002	−0.657	−0.672	−0.656	−0.659	−0.659
C_2–H	0.287	0.019	0.291	0.289	0.250	0.249	0.247
C_4–H	0.257	*−0.021*	0.256	0.253	0.260	0.312	0.313
C_5–H	0.256	*−0.021*	0.258	0.254	0.312	0.259	0.314

[a] $\Delta q = q$(front-meth-a) − q(cation-a). [b] Italicised values indicate sites that have a significant increase in negative charge after formation of the ion pair.

$NH_3\cdots Cl^-$ is −0.942 and −0.970*e*, respectively (at the B3LYP/6-31++G(d,p) level).

Although the changes in charge on any individual atom may be quite small, the combined effect is more significant. The dipole moment of the resultant ion pair is large, and varies between 12.3 and 17.4 debye (Table 4). The charge distribution is also fluid. The electrostatic potential of the dimers has been mapped onto a density isosurface for four of the dimers (Figure 8). When the Cl^- anion is positioned to the side of the ring (meth-side or but-side) the imidazolium is more heavily polarised. The butyl chain remains essentially neutral, except when the Cl^- anion is positioned on the methyl side of the ring where it becomes slightly positive. Although the terminal carbon of the butyl chain carries almost as great a negative charge as the halide, it is shielded by the surrounding (positively charged) hydrogen atoms. Recently, a statistical correlation has been found between maxima and minima of the molecular electrostatic potential and the basicity and acidity of molecules.[60] The cation as a whole has a reasonable polarisability and the trace of the polarisability tensor for the cations is about 100. In the liquid phase multiple anions will surround each cation, and hence some of these polarisation effects are likely to cancel each other out. However, in the liquid phase cation and anion alignment can also enhance polarisation and dipole moments.[61–64]

Table 4. Charge transfer from the Cl^- anion to the cation and dipole moments (μ in debye) at the B3LYP and MP2 level using the 6-31++G(d,p) basis set for the $[C_4C_1im]Cl$ conformers.

	Δq_{Cl} B3LYP	μ B3LYP	μ MP2
front-meth-a	0.165	12.29	12.55
front-meth-b	0.164	12.09	12.26
front-meth-c	0.163	12.59	12.59
front-but-a	0.160	12.46	12.82
front-but-c	0.162	12.46	12.83
top	0.149	9.53	9.02
but-side-a	0.123	16.05	16.27
but-side-b	0.133	16.18	16.41
meth-side-a	0.137	17.49	17.55
meth-side-b	0.137	17.06	17.08
back-a	0.072	17.36	17.60

Analysis of the electron density: Changes in the electron density relative to a promolecule consisting of spherical atoms are shown in Figure 9 for a cut 1.0 and 1.5 Å below the molecular plane of the frontmeth-b (lowest-energy) dimer. The electron distribution is essentially symmetrical. There is a clear depletion of electron density around C^2, and a strong build up of electron density between C^4 and C^5. Such a concentration of electron density will be repulsive to an approaching anion, hence the high energy associated with the back conformer ($\approx +60\ kJ\,mol^{-1}$) and the longer hydrogen bonds associated with the $C^{4/5}$–H atoms in the meth-side and but-side isomers ($\approx +30\ kJ\,mol^{-1}$). This effect may explain why a high probability is found for the Cl^- anion occupying the back position (between C^4 and C^5) in several classical studies, but not experimentally, especially if the $C^{4/5}$ atoms have been assigned positive charges.[28,37,65]

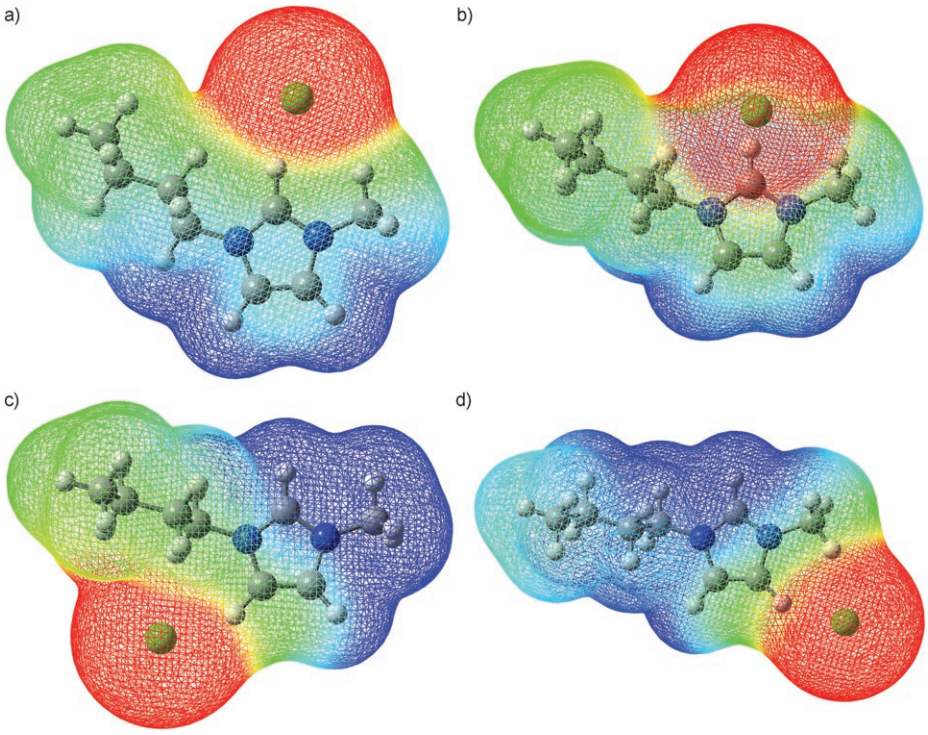

Figure 8. B3LYP/6-31++G(d,p) electrostatic potential mapped onto the 0.0004 density isosurface for the front-meth-a (a), top (b), but-side-a (c) and meth-side-a (d) dimers. The scale spans −0.05 (red) through 0.0 (green) to +0.05 (blue).

Bonding analysis: According to the NBO analysis, electron transfer from the Cl^- anion to the imidazolium cation does not occur through a π-type interaction (occupied Cl p_π HOMO donating into a π* LUMO on the ring), but through a σ-type interaction with a $\sigma^*_{C\text{-}H}$ orbital (the specific orbital is dependent on the position of the Cl^- anion). The delocalised HOMO and HOMO−1 of the dimer (Figure S2 in the Supporting Information) also exhibit no significant π-based interactions. On forming the ion pair, electron density in the π system is indirectly increased and polarised away from the Cl^- anion; for example, when the Cl^- anion is in a front position the occupa-

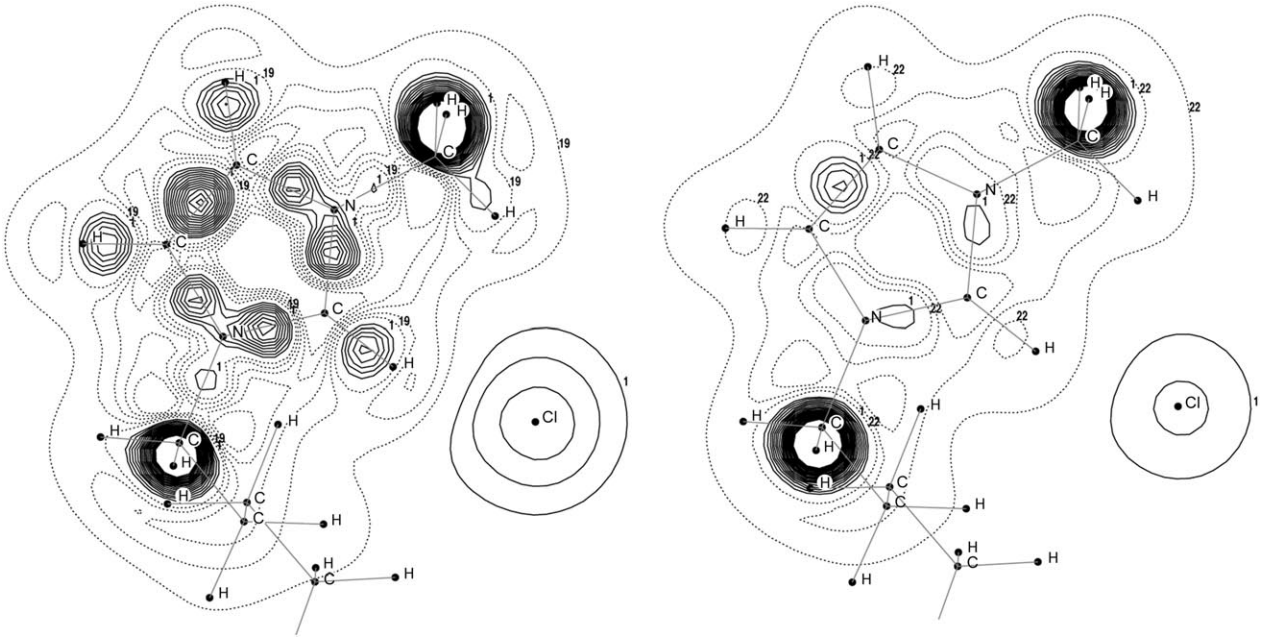

Figure 9. Density contours (intervals 0.025) for frontmeth-b $[C_4C_1im]Cl$ at 1.0 Å (left) and 1.5 Å (right) above the plane of the ring to show the build up (solid lines) and depletion (dashed lines) of electron density relative to a promolecule consisting of spherical atoms.

tion of the closer $\pi_{C=N}$ and $\pi^*_{C=N}$ orbitals decreases while that of the more distant $\pi_{C=C}$ and $\pi^*_{C=C}$ orbitals increases. For each possible position of the Cl^- anion, the N atom with the lone pair varies and is always the one furthest from the Cl^- anion; for the front structure this is N^1, and not N^3 as in the isolated cation. For each conformer the negative charge on the nitrogen atom closest to the Cl^- anion is slightly greater. Electron density in a lone-pair orbital will repulsively interact with the Cl^- anion, hence some stabilisation is obtained by directing this charge into the lower-energy and more diffusive $\pi_{C=N}$ bond.

In the ion pair, as electrons begin to interact with nuclei from the other molecule an increase in the magnitude of the (stabilising) nuclear–electron component of the total energy occurs. However, as the electron clouds of both species repel each other, and electron transfer populates an antibonding orbital on the cation, a concurrent increase in the magnitude of the (destabilising) electron–electron component of the total energy also occurs. Overall, the attractive Columbic effects dominate and the ion pair is more stable than the separated ions, however, there is a net destabilisation of the covalent component of the electronic structure on forming an ion pair.

Figure 10 shows a possible fragment MO energy diagram (delocalised orbitals) for the HOMO–LUMO region of the dimer, in which the orbital interactions have been roughly broken down into electrostatic and covalent (σ and π) components. The Cl^- anion virtual orbitals are too high in energy to interact, and hence only the three nearly degenerate occupied Cl p atomic orbitals (pAO) are shown. The cation HOMO and LUMO are represented, as well as a high-energy orbital that represents one of the $\sigma^*_{C\text{-}H}$ imidazolium ring orbitals. Plots of the cation-a HOMO and LUMO

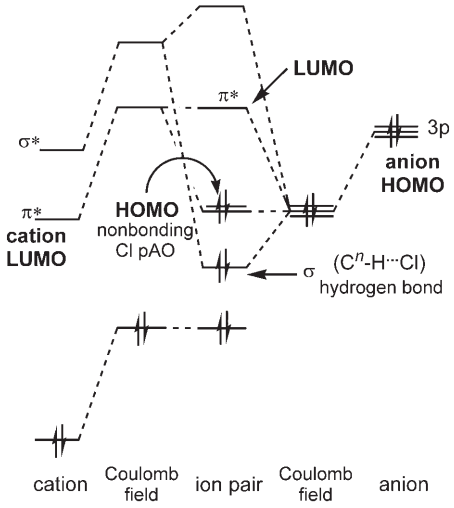

Figure 10. MO energy-level diagram for the interaction of the Cl^- anion with the $[C_4C_1im]^+$ cation to form the $[C_4C_1im]Cl$ dimer.

are shown in Figure 11. These orbitals are the π orbitals that could be expected for any five-membered ring. Notice, however, that there is significant polarisation of the C^2 π component along the C^2–H bond. The bare cation has deep orbitals because of its positive charge, however, on acceptance of electron density from the Cl^- anion this charge is reduced and the orbitals rise in energy. The reverse effect is found for the Cl^- anion.

For dimers in which the Cl^- anion remains in plane with the imidazolium ring, the HOMO (Figure S3a in the Supporting Information) is one of the three Cl^- anion pAOs, and the LUMO (Figure S3b in the Supporting Information) is the cation LUMO. The dimer orbitals are very similar to

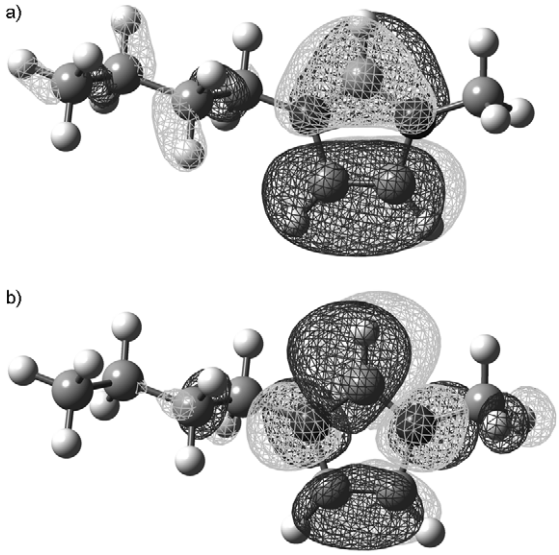

Figure 11. The a) HOMO and b) LUMO of cation-a $[C_4C_1im]^+$. Isosurfaces calculated at 0.02.

the isolated cation orbitals, indicating that covalent interactions are minimal. The HOMO−1 is also a Cl^- anion pAO. The HOMO−2, however, has σ-type symmetry and exhibits interaction between a formally empty C^2–H σ*-bond orbital and the filled pAO on the Cl^- anion (Figure 12). Examination of the orbital coefficients shows that the hydrogen orbital contribution is in phase with, and highly polarised toward, the Cl^- anion contribution. The HOMO−2 also shows a clear contribution from the C^2 pAO, which reinforces our earlier conclusion that the whole C–H unit (and not just the H atom) is important in the formation of a hydrogen bond. Bühl et al. found orbitals of a similar nature when examining the maximised Wannier functions of the Cl lone pairs in a periodic system.[41] The cation HOMO becomes the HOMO−3 of the dimer. For dimers in which the Cl^- anion lies above or below the imidazolium ring, the HOMO and HOMO−3 orbitals differ from those just described. These orbitals exhibit a bonding and antibonding couple composed of an interaction between Cl pAOs and the cation HOMO (Figure 13).

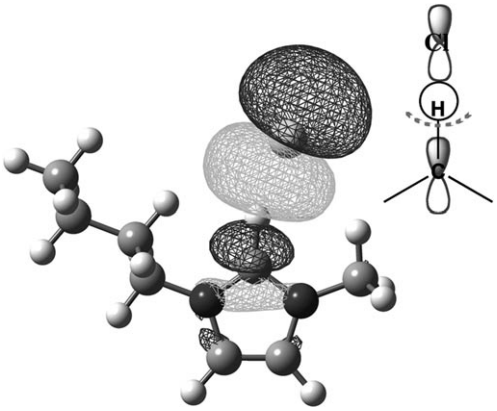

Figure 12. HOMO−2 of frontmeth-a $[C_4C_1im]Cl$ MO. Isosurface calculated at 0.02.

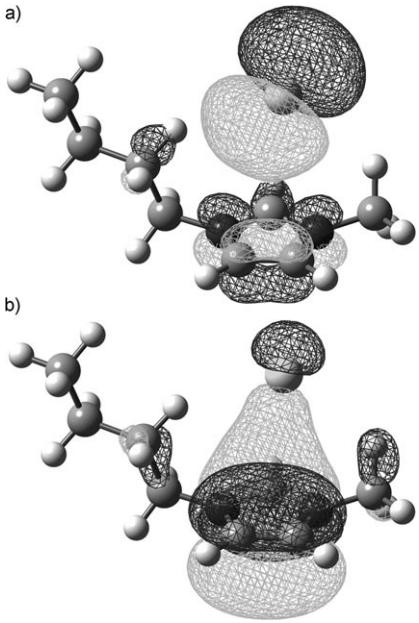

Figure 13. a) HOMO and b) HOMO−3 of top $[C_4C_1im]Cl$ MOs, isosurfaces calculated at 0.02.

Consolidation: The association of the Cl^- anion with the cation is driven by strong attractive Coulombic forces; electronic effects, as we have shown, are destabilising. The large positive charge of the C^n–H units facilitates cation–anion association and the energy gained is substantial (the binding energy of these dimers is $\approx 370\ kJ\,mol^{-1}$). However, the covalent part of the hydrogen bond involves high-energy C^{ring}–H σ* orbitals on the imidazolium and adding electrons to the essentially antibonding π-type LUMO. Indeed, in the crystal structures of $[C_2C_1im][AsF_6]$ and $[C_2C_1im][SbF_6]$, in which no hydrogen bonding has been observed, ring bond lengths are consistently shorter than those in $[C_4C_1im]Cl$.[21,23,66] In terms of general reactivity, any electron density donated to the dimer will "enter" into an antibonding LUMO. The concentrated charge of the Cl^- anion is able to polarise the imidazolium cation, and in the most extreme case may involve formation of a neutral N-heterocyclic carbene through the association of a proton and a Cl^- anion. Thus, in the ionic liquid, the imidazolium cation and Cl^- anion form a very strong ionic hydrogen bond, which is moderated by very minor covalent contributions. We also anticipate that the higher the charge density on the anion the more stabilising the attractive Coulombic interactions will be. This in turn will allow more significant (but destabilising) covalent interactions to occur, and thus stronger hydrogen bonds to form.

Reactivity parameters: One of our aims has been to investigate the physico-chemical properties of $[C_4C_1im]Cl$, including the relative acidity of the ring hydrogen atoms, the hydrogen-bond donating ability (α), the hydrogen-bond acceptor ability (β), and the relative reactivity of the associated carbenes for C^2 versus $C^{4/5}$ coordination.

Relative acidity and hydrogen-bond formation: Why is the hydrogen at C^2 more acidic than those at C^4 or C^5? Why is a Cl^- anion positioned near C^2–H more stable than elsewhere? The NBO analysis predicts very similar charges for these hydrogen atoms, and hence acidity is not simply related to the charge on the hydrogen atoms, but is related to the charge on the whole of the "C^n–H" units. The charge on C^2 is positive while that on $C^{4/5}$ is essentially neutral, and the key difference between these C atoms is that C^2 forms a C=N π bond, leaving it electron deficient, while C^4 and C^5 form a C=C π bond equally sharing the available electrons. The formation of these π bonds has a larger impact than just the charge at the carbon atom. The hydrogen bond formed in the front conformers is stronger than the primary hydrogen bond formed for the but-side or meth-side conformers. This is evidenced by the shorter C^2–H···Cl bond, (2.00 Å) compared with $C^{4/5}$–H···Cl bonds ($\approx$2.17 Å), and the greater stability of this front conformer ($\approx$30 kJ mol^{-1}). The Cl^- anion can approach C^2 closely because there is a depletion of electron density at C^2 (Figure 9) and because C^2–H projects out from between the nitrogen atoms, which, as sites of significant electron density, exert a repulsive force on the approaching negative ion. Moreover, due to a loss of π density at C^2 there is no restriction on the direction of approach. At the rear of the imidazolium ring, however, there is a significant build up of electron-density between C^4 and C^5 (Figure 9), which is repulsive and prevents the Cl^- from approaching too closely, and thus leads to a longer hydrogen bond. The reason the Cl^- anions tend to shift away from a linear hydrogen bond and slightly toward the alkyl groups is to take advantage of regions where there is a local depletion of electron density (Figures 6 and 10). Moreover, the π density of the C=C bond extends above and below the plane of the molecule, restricting the direction of approach for the Cl^- anion to roughly in-plane. Hence there are no $C^{4/5}$ "top" conformers. Coordination of a metal with a partially occupied d manifold at this site should be favoured in terms of overlap (dπ orbitals with the C=C π orbitals) and the greater electron density located at $C^{4/5}$ relative to C^2, thus the N-heterocyclic carbene is more electron donating and we have been able to rationalise the experimental observations of Gründemann et al.[24,25]

Hydrogen-bond donor parameter α: The hydrogen-bond donating ability of $[C_4C_1im]Cl$ is dominated by the cation. C^2–H (+0.54) has more than twice the positive charge of the $C^{4/5}$–H units ($\approx$+0.24) and hence it dominates α. Thus, if the C^2–H position is blocked α decreases. This has been observed experimentally, for example, $[C_4C_1im][BF_4]$ has a higher α value (α=0.627) than the related ionic liquid $[C_4C_1mim][BF_4]$ ($[C_4C_1mim]^+$ is the 1-butyl-2,3-dimethylimidazolium cation; α=0.402).[19]

Recently, the ability of a variety of ionic liquids to act as hydrogen-bond donors using complementary methods has been measured. In solvatochromic experiments using Reichardt's dye as a probe, $[C_4C_1im]^+$-based ionic liquids were shown to be good hydrogen-bond donors with $\alpha\approx$0.62.[19] However, in complementary GC-based experiments using a number of small probe molecules, the same $[C_4C_1im]^+$-based ionic liquids were shown to be poor hydrogen-bond donors.[20] This apparent contradiction can now be resolved. The key difference between these experiments is the charge on the probe molecules: Reichardt's dye has a phenoxide oxygen atom, and all of the probe molecules used in the GC experiment are neutral. Thus, the strong Coulombic driving force is present in the solvatochromic experiment, but not in the GC experiment (here the destabilising forces of covalent hydrogen-bond formation are not compensated for by Coulombic effects). The very poor hydrogen-bond acidities of the ionic liquids in the GC experiment are probably due to the imidazolium cations, which are certainly capable of forming hydrogen bonds, preferentially hydrogen bonding to the ionic liquid anions (because they are anions), and thus are unavailable to the neutral probe molecules. Hence the hydrogen-bond capability of the ionic liquid appears to be large in the solvatochromic experiment, but small in the GC experiment. This type of competition for the hydrogen-bonding sites of the cation has also been evoked to explain the selectivity of Diels–Alder reactions.[67]

The anion has also been observed to have an effect on hydrogen-bond acidity, although this is small by comparison with the effect of the cation.[19] Different anions will alter the strength of the Coulomb field around the cation, changing the polarisation of the cation and hence the energy of the C^{ring}–H σ^* orbitals and the α value.

Hydrogen-bond acceptor parameter β: The ability of an ion-pair dimer to act as a hydrogen-bond acceptor is governed by the energy and shape of the HOMO, which is a Cl pAO. The Cl^- anion remains exposed on the periphery of the imidazolium cation, moreover, the shape of the Cl^- anion HOMO and almost degenerate HOMO−1 are essentially unaffected by covalent bonding to the cation, and thus the Cl^- anion is available to form associations with solute hydrogen-bond donors. In the solid and liquid phases, all of the essentially degenerate Cl^- anion pAOs hydrogen bond to different imidazolium cations, indeed, in the crystal structure of $[C_4C_1im]Cl$ at least three short contacts have been noted, and results from neutron diffraction experiments imply multiple hydrogen-bond interactions.[21,23,65] More generally, the more dense the HOMO lone pair, and the greater the ability of the anion to reorientate (and thus facilitate hydrogen-bond formation), the higher the β value that can be expected for an ionic liquid. For example, $[C_4C_1im][BF_4]$ (β=0.376) has a higher β value than $[C_4C_1im][PF_6]$ (β=0.207),[19] which will have a more diffuse HOMO and more mass to move when reorienting. $[C_4C_1im]Cl$ is expected to

have an even higher β value. The electrostatic potential generated by the cation has a minor effect on the position of the anion HOMO, and thus a small effect on β, for example, the β value of $[C_4C_1mim][BF_4]$ (0.363) is smaller than that of $[C_4C_1im][BF_4]$ (0.376).

Redox properties and reactivity toward solutes: The ability of the ion-pair to accept electrons is governed by the energy and shape of the LUMO orbital, which is the cation LUMO. This is an antibonding orbital and the cation will be electronically destabilised by further electron acceptance, hence the ionic liquid will be unreactive toward solvated species wanting to donate electrons. In addition, a strong external potential will be required to force electron acceptance. The ability of the ion-pair to donate electrons is governed by the energy and shape of the HOMO orbital, which is the anion HOMO. The Cl^- anion however, is a closed-shell species and unwilling to give up electrons, hence the ionic liquid will be unreactive toward solvated species wanting to accept electrons, and will require a strong external potential before electrons can be withdrawn.

Partial charges used for the $[C_4C_1im]^+$ cation in classical models: Table 5 lists the charge distributions used in several recently published classical simulations. There is clearly a large discrepancy in the charges associated with the nitrogen atoms of the ring ranging from $-0.4e$ through essentially neutral to $+0.15e$. The charge on C^2 ranges from $-0.11e$ through essentially neutral to $+0.6e$, and there is significant variation among the charges for the C^2–H, C^4–H and C^5–H hydrogen atoms. The classical models developed to study ionic liquids need to recover the average effects of charge transfer and polarisation in the molecular liquid. Normally the detailed electronic character of the interior of a molecule is not thought to be especially significant in a classical simulation. However, there may be problems in the case of ionic liquids, because the constituent species are highly charged, resulting in large partial charges, the relative position of which may be important. Hence, these differences in partial charges may be significant, and may lead to artefacts in the classical description of phenomena.[39,41,57] Ab initio calculations that include correlation combined with a NAO analysis can be used as a reference for the electronic structure of the gas-phase ion pair.

Variation in derived partial charges can be introduced in a number of ways, when different analysis methods are used, when the same method is used, but different densities or electrostatic potentials (ESP) are input (for example CHelpG on HF-, B3LYP- or MP2-derived), and when different structures (which generate different ESPs and densities) are used. Classical calculations are usually based on charges determined from the ESP such as CHelpG (charges from the electrostatic potential)[70] and RESP (restraint electrostatic potential fit).[71] Ab initio population analysis methods such as Mulliken partition the charge density, as does the DMA (distributed multipole analysis)[72,73] method. ESP-based methods (RESP and CHelpG) are well known to under-determine charges on the interior atoms in a molecule.[74,75] Whereas density-based methods are known to be basis-set dependent. Unlike the Mulliken analysis, the NAO analysis has been shown to exhibit good convergence and stability with respect to basis sets, including those with polarisation and diffuse functions.[74] When using ESP-based methods, the HF/6-31G(d) ESP is a popular choice because the overestimation of polarity brings charges into line with those that could be expected for the same molecule in the liquid phase, moreover, the ESP is expected to be close to convergent, and the calculation is easily accomplished.[75] In order to make a comparison with ESP-based charges, we have determined the Mulliken and NAO charges for the $[C_4C_1im]^+$ cation (Table 6).

We believe the Mulliken charge distribution at the B3LYP level with an extended basis set is unreasonable (Figure 14; compare this with Figure 4). The Mulliken charges indicate the imidazolium ring is neutral while substantial positive charge is relocated onto the alkyl chain. This is not consistent with the resonance structures of Figure 1 or the expectation, and experience, that alkyl chains are neutral

Table 5. Charges used in classical dynamics models (a to g); all are based on 1-alkyl-3-methylimidazolium.[a]

	a[28,68] $[C_2C_1im]$	b[37] $[C_4C_1im]$	c[36,69] $[C_4C_1im]$	d[39] $[C_4C_1im]$	e[38] $[C_nC_1im]$	f[27] $[C_4C_1im]$	g[30] $[C_4C_1im]$
geometry	HF 6-31G(d,p)	HF 6-31G(d,p)	UHF 6-31G(d)	HF 6-31+G(d)	HF 6-31G(d)	HF 6-31G(d)	B3LYP 6-311+G(d)
ESP or $\rho(r)$	MP2 6-31G(d,p)	MP2 6-311G(d)	UHF 6-31G(d)	HF 6-31+G(d)	MP2 cc-pVTZ(-f)	HF 6-31G(d)	B3LYP 6-311+G(d)
partial charges	DMA	Mulliken	RESP	RESP	CHelpG	CHelpG	CHelpG
N_1	−0.267	−0.394	0.0456	0.0682	0.15	0.071	0.111
N_3	−0.267	−0.400	0.0615	0.0596	0.15	0.133	0.133
C_2	0.407	0.5999	0.0076	−0.0055	−0.11	0.229	0.056
C_4	0.105	0.2516	−0.1262	−0.1426	−0.13	0.041	−0.141
C_5	0.105	0.2243	−0.1269	−0.2183	−0.13	0.096	−0.217
C_6	0.124	0.3448	−0.1536	−0.0846	−0.17	0.217	−0.157
C_7	0.130	0.2671	−0.0700	−0.0153	−0.17	0.024	0.095
C_2–H	0.097	UA	0.2305	0.2258	0.21	UA	0.177
C_4–H	0.094	UA	0.2313	0.2340	0.21	UA	0.181
C_5–H	0.094	UA	0.2692	0.2633	0.21	UA	0.207
C_6–H	0.064	UA	0.1271	0.1085	0.13	UA	variable
C_7–H	0.055	UA	0.0975	0.0796	0.13	UA	variable

[a] UA = united atom model; cc-pVTZ(-f) is a cc-pVTZ basis set with all the f functions removed.

Table 6. Selected charges from the Mulliken (M) and natural atomic orbital (NAO) analysis of the $[C_4C_1im]^+$ cation.[a]

	B3LYP NAO	B3LYP M	HF NAO	HF M
N_1	−0.341	−0.089	−0.420	−0.594
N_3	−0.348	−0.060	−0.425	−0.591
C_2	0.268	−0.030	0.378	0.397
C_4	−0.039	−0.070	−0.018	0.022
C_5	−0.035	−0.003	−0.015	0.026
C_6	−0.449	−0.206	−0.404	−0.312
C_7	−0.241	−0.301	−0.199	−0.144
C_{10}	−0.661	−0.658	−0.636	−0.485
C_2–H	0.268	0.205	0.264	0.311
C_4–H	0.278	0.184	0.271	0.300
C_5–H	0.277	0.167	0.271	0.299

[a] B3LYP calculations were carried out with a 6-31++G(d,p) basis set. HF density was calculated by using a 6-31G(d) basis set at the MP2 geometry. B3LYP densities were computed by using the optimised lowest-energy B3LYP structure (cation-a). HF and MP2 densities were computed by using the lowest-energy MP2-optimised structure (cation-c).

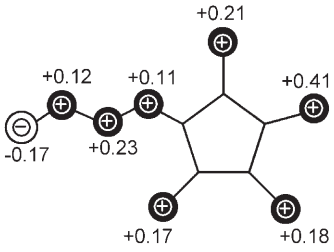

Figure 14. Charge pattern from the Mulliken analysis of the $[C_4C_1im]^+$ cation computed from the B3LYP/6-31++G(d,p) electron density. The specified alkyl charges are methylene and methyl group charges (not atomic charges). No charge indicates an essentially neutral group.

and thus hydrophobic. Basis-set sensitivity is a known problem for the Mulliken analysis, and charges are known to become unphysical when large basis sets with diffuse functions are employed.[74] However, this generates a catch-22 situation as larger basis sets are mandatory for ab initio calculations trying to describe negative ions (such as the Cl^- anion here), or for calculations that include dispersion and correlation effects (which are important for the aromatic imidazolium ring). Furthermore, studies attempting to statistically correlate Mulliken charges with properties such as hydrogen-bond donor ability or polarisability have found, in contrast to NAO charges, no correlation.[59,76] Unlike the Mulliken partial charges computed with a large basis set, the HF/6-31G(d) density partial charges are more polarised than, but remain qualitatively similar to, MP2/6-31++G(d,p) density NAO charges. The Mulliken charges in Table 5 are derived from a HF/6-31G(d,p) optimised structure[31] and MP2/6-311G(d) density[37] and are united atom models and so must be compared to a sum of charges, for example (MP2/NAO) $q(C^4–H)=0.202$, $q(C^5–H)=0.200$ and $q(C^2–H)=0.499$. Thus, these two sets of partial charges are qualitatively consistent.

Of the charge distributions presented in Table 5 those used by Lynden-Bell et al. are the most consistent with the NAO analysis. Nevertheless, compared with the NAO analysis the positive charge determined for C^2 is possibly overemphasised, which may lead to an artificial preference for interaction of an anion with C^2 or C^2–H. Lopes et al. commented that the charges employed by Lynden-Bell et al. are significantly different in both size and magnitude compared with theirs and other authors.[38]

A comparison of the HF/6-31G(d) partial charges determined here (Table 6) and those from the RESP and CHelpG methods (Table 5) show that method plays a dominant role. For example, for the nitrogen atoms, the RESP method predicts an essentially neutral charge, the CHelpG method predicts a positive charge and all of the density-based methods predict a negative charge (thus imparting a certain validity to this particular charge distribution). Basis-set effects play a secondary role for this range of methods. Differences in partial charges have not generally led to substantial discrepancies in computed thermodynamic properties, however, care has to be made in interpreting atomic-scale phenomena that do depend on local partial charges, for example, conformational changes and atom–atom interactions.[77] There is also evidence that partial charges impact on interfacial phenomena. For example, attempts to mimic anion to cation electron transfer by reducing the overall charge on the ionic species has resulted in a significant impact on mixing dynamics at the IL/water interface.[49]

In addition, the structure chosen can affect the charge distribution, and it has recently been determined that multiple low-energy conformers exist for $[C_4C_1im]Cl$ dimers. We have found that partial charges and the electrostatic potential do not vary significantly with butyl chain rotation, but they do vary with the position of the anion (Table 3, Figure 8). The issue of which particular conformer to use can be avoided by taking an average structure, or eliminated through explicit symmetrisation and restriction of charges. Indeed, several recent IL simulations have used charges averaged over a small number of structures, however, this raises new problems.[35,38,75]

Conclusion

An examination of the electronic structure and orbital interactions obtained from ab initio calculations has enabled us to provide viable explanations for a number of experimentally observed phenomena: the hydrogen-bond donor and acceptor abilities of the imidadazolium-based ionic liquids, the relative acidity of hydrogen atoms in the imidazolium ring, the low probability of finding a Cl^- anion at the rear of an imidazolium ring, and the expansion of the imidazolium ring in the presence of strong hydrogen-bond acceptors. The unreactive but coordinating environment and large electrochemical window of the ionic liquid have been accounted for and the strong electron-donating character of $C^{4/5}$ in imidazolylidene chemistry has been rationalised.

The electronic structure of the $[C_4C_1im]^+$ cation is best represented by a double bond between C^4 and C^5 and a de-

localised 3c-4e contribution across N^1-C^2-N^3, however, there is also extensive delocalisation around the entire ring. The charge distribution determined by the NAO analysis for the cation is not intuitive; the peripheral hydrogen atoms carry most of the positive charge and all of the carbon atoms, except C^2, which is substantially positive, carry a negative charge. Moreover, the formally positive nitrogen atoms carry significant negative charge. The details of the charge distribution within the imidazolium cation differ depending on the position of the associated Cl^- anion, and reflect a substantial polarisability for the imidazolium cation. The partial charge models used in a number of classical simulations were examined, and the model used by Lynden-Bell et al. was found to be consistent with the NAO analysis reported here.

We have demonstrated that the hydrogen bond is primarily ionic with a moderate covalent character. Analysis of the charge distribution, molecular orbitals and electron density of the dimer complex $[C_4C_1im]Cl$ revealed that Coulombic attraction is the dominant stabilising force. A small quantity of electron density is transferred to the cation, principally through the weak covalent component that involves high-energy C^{ring}–H σ* orbitals and destabilisation of the imidazolium ring. The formation of a covalent hydrogen bond must be compensated for by a strong and stabilising ionic interaction. The Cl^- anion is repelled from local areas of build up in electron density, particularly the π density associated with nitrogen lone pairs and the C^4–C^5 double bond. This stops the Cl^- ion from approaching too closely and forming strong hydrogen bonds especially with the $C^{4/5}$–H moieties. The large positive charge at the "C^2–H" unit, and the repulsive interactions due to the C=C bond, rationalise both the observed higher acidity of C^2–H, and the better electron-donating properties at $C^{4/5}$. The Cl^- anion is still highly anionic, and dominates the ion-pair HOMO. Compared with larger less mobile and more diffuse anions, the Cl^- anion is expected to favour accepting further hydrogen bonds, but will not release significantly more charge. The ion-pair LUMO is the cation antibonding LUMO and thus electron acceptance is not favourable. The interactions governing the top conformers, however, are very different from those in which the Cl^- anion remains in plane. In this case, the Cl^- anion interacts with the π manifold of orbitals. Thus, based on an analysis of the electronic structure of a gas-phase ion pair we have been able to rationalise some of the experimentally observed properties of the imidazolium-based ionic liquids.

Computational Methods

MP2 and DFT calculations using Becke's three-parameter exchange functional[78] in combination with the Lee, Yang and Parr correlation functional[79] (B3LYP) have been carried out with a 6-31G++G(d,p)[80–82] basis set as implemented in the GAUSSIAN 03 suite of programs.[83] Structures have been fully optimised, under no symmetry constraints, and the B3LYP structures confirmed by frequency analysis. Details of the optimisation procedures and structures obtained are reported elsewhere.[56] Overall, the B3LYP functional combined with a 6-31++G(d,p) basis set was found to be adequate for determining gross energy differences, however, the method was found to be incapable of recovering the correct energy ordering for structures that differ subtly because of torsional motion in the butyl chain, or because of significant dispersion. In this case MP2/6-31++G(d,p) level calculations offer a better alternative.[56] An extended basis set is necessary to obtain a good electron density for analysis. Polarisation functions are desirable due to the highly polarisable imidazolium cation, diffuse functions are required to adequately describe negative ions, and it is advisable to include polarisation functions on the hydrogen atoms involvde in hydrogen bonding. Population analysis was carried out by using the methods implemented in GAUSSIAN 03. Natural atomic orbital (NAO) and natural bond orbital (NBO) analyses (version 3) of selected conformers have been carried out.[84–88] Electron density maps and the Laplacian contours were produced with the program MOLDEN.[89]

Acknowledgements

P. Hunt gratefully acknowledges The Royal Society for a University Research Fellowship.

[1] P. Wasserscheid, K. Wilhelm, *Angew. Chem.* **2000**, *112*, 3926; *Angew. Chem. Int. Ed.* **2000**, *39*, 3772.
[2] T. Welton, *Chem. Rev.* **1999**, *99*, 2071.
[3] T. Welton, P. Wasserscheid, *Ionic Liquids in Synthesis*, Wiley-VCH, Weinheim, **2002**.
[4] J. D. Holbrey, K. R. Seddon, *Clean Products and Processes, Vol. 1*, Springer, Heidelberg, **1999**, p. 223.
[5] T. Welton, *Coord. Chem. Rev.* **2004**, *248*, 2459.
[6] A. J. Arduengo, R. L. Harlow, M. Kline, *J. Am. Chem. Soc.* **1991**, *113*, 361.
[7] J. Cioslowski, *Int. J. Quantum Chem. Quantum Chem. Symp.* **1993**, *27*, 309.
[8] C. Boehme, G. Frenking, *J. Am. Chem. Soc.* **1996**, *118*, 2039.
[9] C. Heinemann, T. Müller, Y. Apeloig, H. Schwarz, *J. Am. Chem. Soc.* **1996**, *118*, 2023.
[10] M. Tafiplosky, W. Scherer, K. Öfele, G. Artus, B. Pederson, W. A. Herrman, G. S. McGrady, *J. Am. Chem. Soc.* **2002**, *124*, 5865.
[11] A. M. Magill, B. F. Yates, *Aust. J. Chem.* **2004**, *57*, 1205.
[12] A. M. Magill, K. J. Cavell, B. F. Yates, *J. Am. Chem. Soc.* **2004**, *126*, 8717.
[13] A. J. Arduengo, H. V. Dias, R. L. Harlow, M. Kline, *J. Am. Chem. Soc.* **1992**, *114*, 5530.
[14] A. J. Arduengo, H. V. Rasika Dias, D. A. Dixion, R. L. Harlow, W. T. Klooster, T. F. Koetzle, *J. Am. Chem. Soc.* **1994**, *116*, 6812.
[15] M. J. Kamlet, R. W. Taft, *J. Am. Chem. Soc.* **1976**, *98*, 377.
[16] R. W. Taft, M. J. Kamlet, *J. Am. Chem. Soc.* **1976**, *98*, 2886.
[17] T. Yokoyama, R. W. Taft, M. J. Kamlet, *J. Am. Chem. Soc.* **1976**, *98*, 3233.
[18] M. J. Kamlet, J. L. Abboud, R. W. Taft, *J. Am. Chem. Soc.* **1977**, *99*, 6027.
[19] L. Crowhurst, P. R. Mawdsley, J. M. Perez-Arlandis, P. A. Salter, T. Welton, *Phys. Chem. Chem. Phys.* **2003**, *5*, 2790.
[20] J. L. Anderson, J. Ding, T. Welton, D. W. Armstrong, *J. Am. Chem. Soc.* **2002**, *124*, 14247.
[21] S. Saha, S. Hayashi, A. Kobayashi, H. Hamaguchi, *Chem. Lett.* **2003**, *32*, 740.
[22] A. G. Avent, P. A. Chaloner, M. P. Day, K. R. Seddon, T. Welton, *J. Chem. Soc. Dalton Trans.* **1994**, 3405.
[23] J. D. Holbrey, W. M. Reichert, M. Nieuwenhuyzen, S. Johnston, K. R. Seddon, R. D. Rogers, *Chem. Commun.* **2003**, 1636.
[24] S. Gründemann, A. Kovacevic, M. Albrecht, J. W. Faller, R. H. Crabtree, *Chem. Commun.* **2001**, 2274.
[25] A. Kovacevic, S. Gründemann, J. R. Miecznikowski, E. Clot, O. Eisenstein, R. H. Crabtree, *Chem. Commun.* **2002**, 2580.

[26] A. R. Chianese, A. Kovacevic, B. M. Zeglis, J. W. Faller, R. H. Crabtree, *Organometallics* **2004**, *23*, 2461.
[27] J. K. Shah, J. F. Brennecke, E. J. Maginn, *Green Chem.* **2002**, *4*, 112.
[28] C. G. Hanke, S. L. Price, R. M. Lynden-Bell, *Mol. Phys.* **2001**, *99*, 801.
[29] J. de Andrade, E. S. Böes, H. Stassen, *J. Phys. Chem. B* **2002**, *106*, 3546.
[30] T. I. Morrow, E. J. Maginn, *J. Phys. Chem. B* **2002**, *106*, 12807.
[31] C. J. Margulis, H. A. Stern, B. J. Berne, *J. Phys. Chem. B* **2002**, *106*, 12017.
[32] C. J. Margulis, *Mol. Phys.* **2004**, *102*, 829.
[33] R. M. Lynden-Bell, *Mol. Phys.* **2003**, *101*, 2625.
[34] S. Alavi, D. L. Thompson, *J. Chem. Phys.* **2005**, 122, 154704.
[35] C. Cadena, J. L. Anthony, J. K. Shah, T. I. Morrow, J. F. Brennecke, E. J. Maginn, *J. Am. Chem. Soc.* **2004**, *126*, 5300.
[36] J. de Andrade, E. S. Böes, H. Stassen, *J. Phys. Chem. B* **2002**, *106*, 13344.
[37] S. Urahata, M. Ribeiro, *J. Chem. Phys.* **2004**, *120*, 1855.
[38] J. Lopes, J. Deschamps, A. Padua, *J. Phys. Chem. B* **2004**, *108*, 2038.
[39] Z. Liu, S. Haung, W. Wang, *J. Phys. Chem. B* **2004**, *108*, 12978.
[40] M. G. Del Popolo, G. A. Voth, *J. Phys. Chem. B* **2004**, *108*, 1744.
[41] M. Bühl, A. Chaumont, R. Schurhammer, G. Wipff, *J. Phys. Chem. A* **2005**, *109*, 18591.
[42] W. R. Carper, G. J. Mains, B. J. Piersma, S. W. Mansfield, C. K. Larive, *J. Phys. Chem.* **1996**, *100*, 4724.
[43] G. J. Mains, E. A. Nantsis, W. R. Carper, *J. Phys. Chem. A* **2001**, *105*, 4371.
[44] L. P. Davis, C. J. Dymek, J. P. Stewart, H. P. Clark, W. J. Lauderdale, *J. Am. Chem. Soc.* **1985**, *107*, 5041.
[45] M. Blander, E. Bierwagen, K. G. Calkins, L. A. Curtiss, S. L. Price, M. Saboungi, *J. Chem. Phys.* **1992**, *97*, 2733.
[46] S. Takahashi, L. A. Curtiss, D. Gosztola, N. Koura, M. Saboungi, *Inorg. Chem.* **1995**, *34*, 2990.
[47] S. Takahashi, K. Suzuya, S. Kohara, N. Koura, L. A. Curtiss, M. Saboungi, *Z. Phys. Chem.* **1999**, *209*, 209.
[48] J. K. Shah, E. J. Maginn, *Fluid Phase Equilib.* **2004**, *222–223*, 195.
[49] A. Chaumont, G. Wipff, *Inorg. Chem.* **2004**, *43*, 5891.
[50] Z. Meng, A. Dölle, W. R. Carper, *THEOCHEM.* **2002**, *585*, 119.
[51] E. A. Turner, C. C. Pye, R. D. Singer, *J. Phys. Chem. A* **2003**, *107*, 2277.
[52] F. C. Gozzo, L. S. Santos, R. Augusti, C. S. Consorti, J. Dupont, M. N. Eberlin, *Chem. Eur. J.* **2004**, *10*, 6187.
[53] E. R. Talaty, S. Raja, V. J. Storhaug, A. Dölle, W. R. Carper, *J. Phys. Chem. B* **2004**, *108*, 13177.
[54] Y. U. Paulechka, G. J. Kabo, A. V. Blokhin, A. O. Vydrov, J. W. Magee, M. Frenkel, *J. Chem. Eng. Data* **2003**, *48*, 457.
[55] Y. Wang, H. Li, S. Han, *J. Chem. Phys.* **2005**, *123*, 174501.
[56] P. A. Hunt, I. R. Gould, *J. Phys. Chem. A* **2006**, *110*, 2269.
[57] M. G. Del Popolo, R. M. Lynden-Bell, J. Kohanoff, *J. Phys. Chem. B* **2005**, *109*, 5895.
[58] B. L. Bhargava, S. Balasubramanian, *Chem. Phys. Lett.* **2006**, *417*, 486.
[59] J. A. Platts, *Phys. Chem. Chem. Phys.* **2000**, *2*, 973.
[60] O. Lamarche, J. A. Platts, *Phys. Chem. Chem. Phys.* **2003**, *5*, 677.
[61] B. Kirchner, J. Hutter, *J. Chem. Phys.* **2004**, *121*, 5133.
[62] D. Barker, M. Sprik, *Mol. Phys.* **2003**, *101*, 1183.
[63] P. L. Silvestrelli, M. Parrinello, *Phys. Rev. Lett.* **1999**, *82*, 3308.
[64] P. L. Silvestrelli, M. Parrinello, *J. Chem. Phys.* **1999**, *111*, 3572.
[65] C. Hardacre, J. D. Holbrey, S. E. McMath, D. T. Bowron, A. K. Soper, *J. Chem. Phys.* **2003**, *118*, 273.
[66] K. Matsumoto, R. Hagiwara, R. Yoshida, Y. Ito, Z. Mazej, P. Benkic, B. Zemva, O. Tamada, H. Yoshino, S. Matsubara, *Dalton Trans.* **2004**, 144.
[67] A. Aggarwal, N. L. Lancaster, A. Sethi, T. Welton, *Green Chem.* **2002**, *4*, 517.
[68] J. B. Harper, R. M. Lynden-Bell, *Mol. Phys.* **2004**, *102*, 85.
[69] A. Chaumont, G. Wipff, *J. Phys. Chem. B* **2004**, *108*, 3311.
[70] C. M. Breneman, K. B. Wiberg, *J. Comput. Chem.* **1990**, *11*, 361.
[71] D. A. Case, T. A. Darden, T. E. Cheatham, III, C. L. Simmerling, J. Wang, R. E. Duke, R. Luo, K. M. Merz, B. Wang, D. A. Pearlman, M. Crowley, S. Brozell, V. Tsui, H. Gohlke, J. Mongan, V. Hornak, G. Cui, P. Beroza, C. Schafmeister, J. W. Caldwell, W. S. Ross, P. A. Kollman, Amber Molecular Dynamics Package, University of California, San Francisco, **2004**.
[72] A. J. Stone, M. Alderton, *Mol. Phys.* **1985**, 56, 1047.
[73] A. J. Stone, M. Alderton, *Mol. Phys.* **2002**, 100, 221.
[74] F. Jensen, *Introduction to Computational Chemistry*, Wiley, Chichester, **1999**, p. 230ff.
[75] W. D. Cornell, P. Cieplak, C. I. Bayly, I. R. Gould, K. M. Merz, D. M. Ferguson, D. C. Spellmeyer, T. Fox, J. W. Caldwell, P. A. Kollman, *J. Am. Chem. Soc.* **1995**, *117*, 5179.
[76] O. Lamarche, J. A. Platts, A. Hersey, *Phys. Chem. Chem. Phys.* **2001**, *3*, 2747.
[77] C. Chipot, C. Millot, B. Maigret, P. Kollman, *J. Phys. Chem.* **1994**, *98*, 11362.
[78] A. D. Becke, *J. Chem. Phys.* **1993**, *98*, 5648.
[79] C. Lee, W. Yang, R. G. Parr, *Phys. Rev. B* **1988**, *37*, 785.
[80] M. M. Francl, W. J. Pietro, W. J. Hehre, J. S. Binkley, D. J. DeFrees, J. A. Pople, M. S. Gordon, *J. Chem. Phys.* **1982**, *77*, 3654.
[81] P. C. Hariharan, J. A. Pople, *Theor. Chim. Acta* **1973**, *28*, 213.
[82] T. Clark, J. Chandrasekhar, G. W. Spitznagel, P. von R. Schleyer, *J. Comput. Chem.* **1983**, *4*, 294.
[83] Gaussian 03, Revision C 01, M. J. Frisch, G. W. Trucks, H. B. Schlegel, G. E. Scuseria, M. A. Robb, J. R. Cheeseman, J. A. Montgomery, Jr., T. Vreven, K. N. Kudin, J. C. Burant, J. M. Millam, S. S. Iyengar, J. Tomasi, V. Barone, B. Mennucci, M. Cossi, G. Scalmani, N. Rega, G. A. Petersson, H. Nakatsuji, M. Hada, M. Ehara, K. Toyota, R. Fukuda, J. Hasegawa, M. Ishida, T. Nakajima, Y. Honda, O. Kitao, H. Nakai, M. Klene, X. Li, J. E. Knox, H. P. Hratchian, J. B. Cross, V. Bakken, C. Adamo, J. Jaramillo, R. Gomperts, R. E. Stratmann, O. Yazyev, A. J. Austin, R. Cammi, C. Pomelli, J. W. Ochterski, P. Y. Ayala, K. Morokuma, G. A. Voth, P. Salvador, J. J. Dannenberg, V. G. Zakrzewski, S. Dapprich, A. D. Daniels, M. C. Strain, O. Farkas, D. K. Malick, A. D. Rabuck, K. Raghavachari, J. B. Foresman, J. V. Ortiz, Q. Cui, A. G. Baboul, S. Clifford, J. Cioslowski, B. B. Stefanov, G. Liu, A. Liashenko, P. Piskorz, I. Komaromi, R. L. Martin, D. J. Fox, T. Keith, M. A. Al-Laham, C. Y. Peng, A. Nanayakkara, M. Challacombe, P. M. W. Gill, B. Johnson, W. Chen, M. W. Wong, C. Gonzalez, J. A. Pople, Gaussian, Inc., Wallingford CT, **2004**..
[84] J. P. Foster, F. Weinhold, *J. Am. Chem. Soc.* **1980**, *102*, 7211.
[85] A. E. Reed, F. Weinhold, *J. Chem. Phys.* **1983**, *78*, 4066.
[86] A. E. Reed, R. B. Weinstock, F. Weinhold, *J. Chem. Phys.* **1985**, *83*, 735.
[87] A. E. Reed, F. Weinhold, *J. Chem. Phys.* **1985**, *83*, 1736.
[88] E. Reed, L. A. Curtiss, F. Weinhold, *Chem. Rev.* **1988**, *88*, 899.
[89] G. Schaftenaar, J. H. Noordik, *J. Comput.-Aided Mol. Des.* **2000**, *14*, 123.

Received: January 23, 2006
Published online: June 28, 2006

